



# An image segmentation for the measurement of microstructures in ductile cast iron

Amelia Carolina Sparavigna

## ► To cite this version:

Amelia Carolina Sparavigna. An image segmentation for the measurement of microstructures in ductile cast iron. Philica, 2017, 2017 (1159). hal-01635665

**HAL Id: hal-01635665**

**<https://hal.science/hal-01635665>**

Submitted on 15 Nov 2017

**HAL** is a multi-disciplinary open access archive for the deposit and dissemination of scientific research documents, whether they are published or not. The documents may come from teaching and research institutions in France or abroad, or from public or private research centers.

L'archive ouverte pluridisciplinaire **HAL**, est destinée au dépôt et à la diffusion de documents scientifiques de niveau recherche, publiés ou non, émanant des établissements d'enseignement et de recherche français ou étrangers, des laboratoires publics ou privés.

## **An image segmentation for the measurement of microstructures in ductile cast iron**

**Amelia Carolina Sparavigna**  
Politecnico di Torino, Torino, Italy

The work is applying an image segmentation to a micrograph which is showing the microscopic structures of a specimen of ductile cast iron. The segmentation allows the measurement of the size of the nodules.

**Keywords:** Image processing, Segmentation of images, Size of domains, Side distribution, Ductile cast iron.

As explained in [1], techniques exist to have quantitative analyses of the metallographic specimens, suitable for researches concerning metals and alloys, but also for non-metallic or composite materials. In these analyses, it is used a specimen in the form of a two-dimensional plane from a three-dimensional sample. Measurements may involve the determination of the apparent diameter of discrete particles that we can see in the specimen. To obtain such a measure, a manual approach can be used, made “with the aid of templates overlaying the microstructure” [1], or with an image processing of the related micrographs. As stressed in Ref. 1, an adequate sampling is necessary to obtain a proper statistical basis for the measurement [1-5]. “Efforts to eliminate bias are required”. Among the basic quantitative investigations, besides the measurements of the size and size distribution of particles, of their shape and of the spacing between them, we find also the measurement of the grain size in polycrystalline materials and the determination of the volume fraction of a phase or constituent.

The measurement of the size and size distribution of particles is the proper task for an image segmentation method that we have recently developed and applied [6-12]. In image processing, a segmentation is a method of partitioning an image into multiple sets of pixels, defined as super-pixels, in order to have a representation, which can be simpler than the original one or more useful to the following desired analyses [13]. Specifically, the segmentation is a process of assigning a label to every pixel in an image, such that the pixels having the same label share certain characteristics [13]. As a consequence, the result of a segmentation is a set of “segments”, or “super-pixels”, or “domains”, that are covering the whole image. The segmentation can also give a set of contours, that is of “edges”, extracted from the image. In this case, the segmentation gives an “edge detection”.

Several methods exist for segmentation, as we can appreciate from [13]. Here we use a segmentation based on a thresholding of gray-scale images [6]. By selecting a suitable threshold, the image is converted into a binary (black and white) image. In several cases, this is enough for evidencing the domains among the black or the white pixels. Details of the method of segmentation are given in [6].

Let us consider the image proposed in [1] and here reproduced in the Figure 1. It is showing a micrograph of ductile iron. This material is also known as ductile cast iron, nodular cast iron, spheroidal graphite iron, spheroidal graphite cast iron, and SG iron [14,15]. It is a type of graphite-rich cast iron discovered in 1943 by Keith Millis [14]. As told in [14], in the Figure 1 we can see the carbon islanding effect around nodules. Actually, from the Figure 1, we can try to determine the nodules distribution, but also the areas surrounding them. Let us start from the nodules and their size distribution.

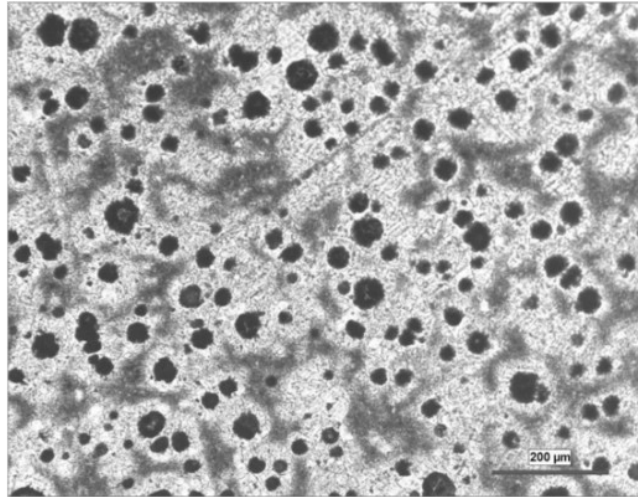


Figure 1: Light optical micrograph of polished and etched ductile iron. Etched in 3% Nital. 100X. Courtesy Michelshock, McGill University, for Wikipedia.

As previously told, the method proposed and applied in [6-12] is based on the thresholding of the gray tones of the image under study, to render it into a binary one. Let us remember that the values of the gray tones are integers ranging from 0 (black) to 255 (white). The histogram of the image is given in the right panel of the Figure 2. We have obtained it by means of the image processing software GIMP.

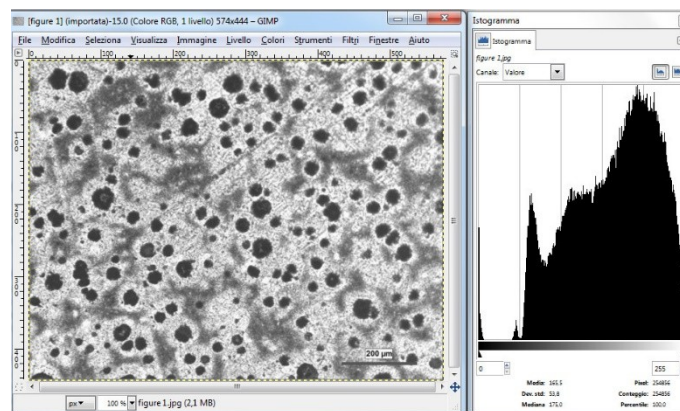


Figure 2: Screenshot of the image and its histogram obtained using GIMP.

At a first glance, the micrograph in the Figure 1 seems being an image having a trimodal histogram, that is, a histogram with three peaks. Actually, as we can see from Fig.2, the histogram has two two evident peaks corresponding to the dark and bright areas, and between then a less pronounced peak for the gray pixels. Let us consider the peak at dark values; we can try to use two thresholds to segment the image in order to have only the pixels pertaining to this peak (for a multilevel thresholding based on the image entropy, see [16]). Using GIMP we can select manually a part of the histogram, for instance, that corresponding to the blue band in the Figure 3. The selection of the gray tones in this blue stripe of the histogram are producing the binary image that we can see in the Figure 3.

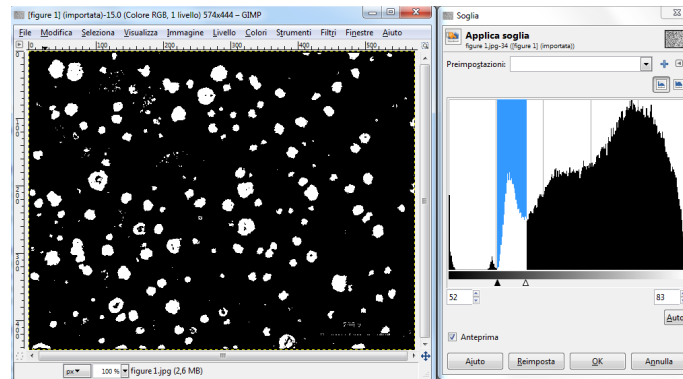


Figure 3: Segmentation of the histogram and of the image for evidencing the nodules.

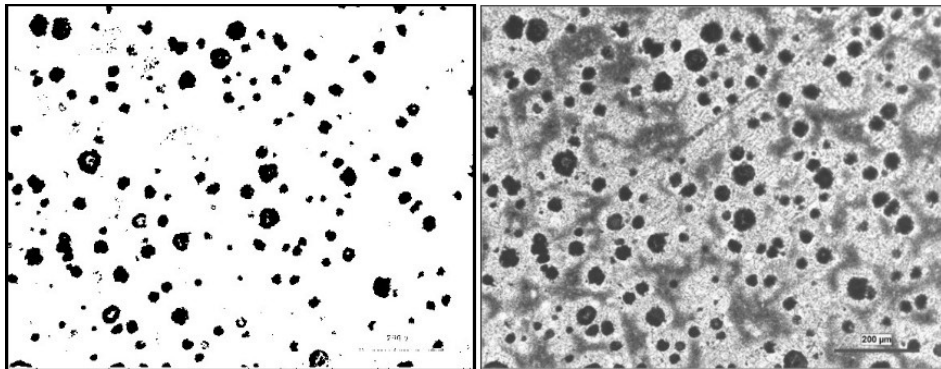


Figure 4. After the segmentation and the inversion of colors, we have the image on the left, that we can compare to the image in the Figure 1.

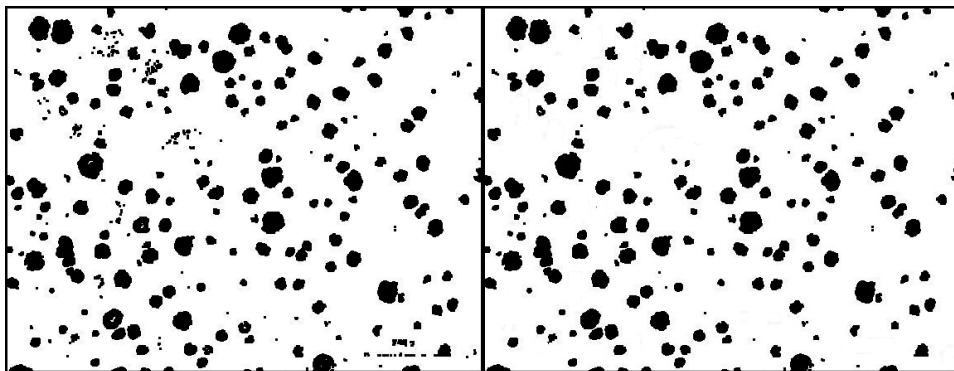


Figure 5: The image on the left is obtained by using the GIMP Dilate filter on the binary image in the Figure 4. This GIMP filter widens and enhances dark areas of the active layer or selection. Using Paint, some spurious black domains are removed (right panel).

Let us invert the tones of the image, obtaining the Figure 4 on the left. We can compare it to the original image. We see that the nodules have their sizes slightly reduced. For this reason, we have to apply some processing before determining the size distribution. We can use the GIMP Dilate filter, which widens and enhances dark areas of the active layer or selection. We obtain the image in the Figure 5 (left panel). Using Paint, we have removed some spurious domains, having the image in Figure 5 (right panel). On this last image, we apply the segmentation [6]. The result is given in the Figure 6, which is showing the black domains as “super-pixels”, each colored by a different color.

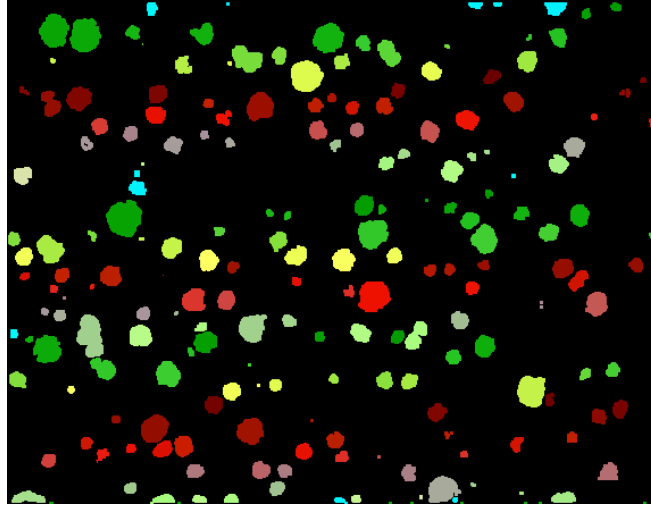


Figure 6: Result of the segmentation of the image in the Figure 1. Each nodule (super-pixel) has a different color.

After having determined the colored domains, it is easy to obtain the cross-section of each of them. The cross-section is given as the number of pixels contained in the domain. If we have the possibility to know the measure, in microns, of the image size, it is very simple to estimate the area (in microns) of the domains. Moreover, we can give the size distribution of the domains, that is, the distribution of the cross-sections of nodules displayed by the micrograph of Figure 1. We obtain the distribution by counting the cross-sections according to their area (in pixels) within intervals spaced of a certain amount of pixels. Here the areas are spaced of 50 pixels, to obtain the distribution given in the Figure 7.

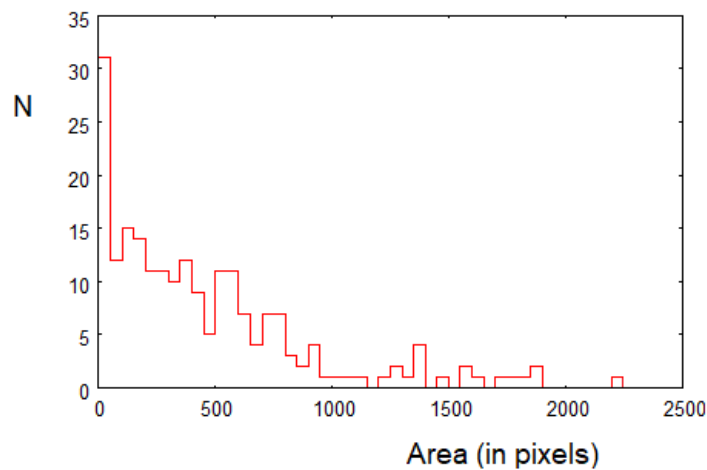


Figure 7: Distribution of the cross-sections of nodules. The areas are spaced in intervals of 50 pixels.

Let us conclude showing how it is possible to evaluate the islanding effect around the nodules. Again, we use the histogram in the Figure 2. As we made for the nodules, we segment the histogram by choosing the highest and broad peak. This selection gives the white domains in the binary image on the left of Figure 8. It is easy to evaluate the percentage of the image covered by the white pixels, by counting the white pixels in it.

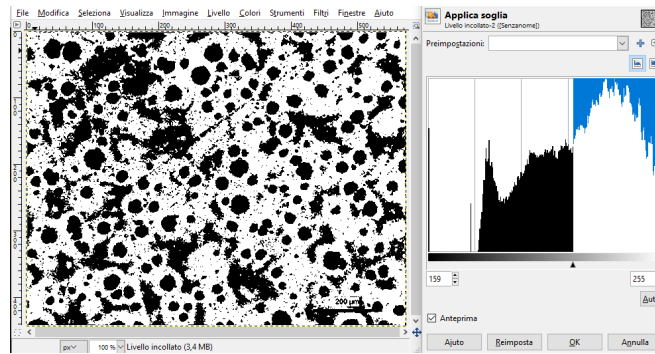


Figure 8: Segmentation of the histogram and of the image for evidencing the islanding effect.

Here we have proposed an approach based on the segmentation described in [6]. Let us conclude remarking that several software and methods exist for the image processing of micrographs for metallography. Some of them are reported in Refs. [17-20].

## References

- [1] Vv. Aa. (2017). Metallography, in Wikipedia, at <https://en.wikipedia.org/wiki/Metallography>
- [2] Geels, K., Fowler, D. B., Kopp, W. U., & Rückert, M. (2007). Metallographic and materialographic specimen preparation, light microscopy, image analysis, and hardness testing (Vol. 46). West Conshohocken, PA: ASTM International. Metallography and Microstructures, Vol. 9, ASM Handbook, ASM International, Materials Park, OH, 2005.
- [3] Voort, G. V. (1984). Metallography: principles and practice. McGraw-Hill Book Company, 1984,, 752.
- [4] Petzow, G. (1978). Metallographic etching: metallographic and ceramographic methods for revealing microstructure. American Society for Metals.
- [5] Bjerregaard, L., Geels, K., Ottesen, B., & Ruckert M. (1992). Metalog guide, 1992. Struers Tech A/S, Denmark.
- [6] Sparavigna, A. C. (2017). Image Segmentation Applied to the Study of Micrographs of Cellular Solids. Int. Journal of Sciences, 6(02), 68-76. DOI: 10.18483/ijSci.1201
- [7] Sparavigna, A. C. (2016). A method for the segmentation of images based on thresholding and applied to vesicular textures. Philica 2016, 889. Available arXiv, <http://adsabs.harvard.edu/abs/2016arXiv161201131S>
- [8] Sparavigna, A. C. (2017). Measuring the particles in fly ash by means of an image segmentation. Philica, n.1105. Available HAL, <https://hal.archives-ouvertes.fr/hal-01579285v1>
- [9] Sparavigna, A. C. (2016). Analysis of a natural honeycomb by means of an image segmentation. Philica, n.897. Available HAL, <https://hal.archives-ouvertes.fr/hal-01416832v1>
- [10] Sparavigna, A. C. (2017). Image segmentation applied to micrographs of microcellular plastics. Philica, n.953. Available HAL, <https://hal.archives-ouvertes.fr/hal-01456692v1>
- [11] Sparavigna, A. C. (2017). Measuring the size of tubules in phloem and xylem of plants. Philica, n.1104. Available HAL, <https://hal.archives-ouvertes.fr/hal-01578826v1>
- [12] Sparavigna, A. C. (2017). Image Segmentation Applied to the Analysis of Fabric Textures. Philica, n.1157. Available HAL, <https://hal.archives-ouvertes.fr/hal-01633061v1>
- [13] Vv. Aa. (2016). Image segmentation, in Wikipedia. [https://en.wikipedia.org/wiki/Image\\_segmentation](https://en.wikipedia.org/wiki/Image_segmentation)
- [14] Vv. Aa. (2017). Ductile iron, in Wikipedia, at [https://en.wikipedia.org/wiki/Ductile\\_iron](https://en.wikipedia.org/wiki/Ductile_iron)
- [15] Smith, W. F., & Hashemi, Javad (2006). Foundations of Materials Science and Engineering (4th ed.), McGraw-Hill, ISBN 0-07-295358-6.
- [16] Sparavigna, A. C. (2015). Tsallis entropy in bi-level and multi-level image thresholding. International Journal of Sciences, 4(1), 40-49.

- [17] Maragos, P. (1987). Tutorial on advances in morphological image processing and analysis. *Optical engineering*, 26(7), 623-632.
- [18] Tewari, A., & Gokhale, A. M. (2000). Application of three-dimensional digital image processing for reconstruction of microstructural volume from serial sections. *Materials Characterization*, 44(3), 259-269.
- [19] Sternberg, S. R. (1986). Grayscale morphology. *Computer vision, graphics, and image processing*, 35(3), 333-355.
- [20] Stampfl, J., Scherer, S., Berchthaler, M., Gruber, M., & Kolednik, O. (1996). Determination of the fracture toughness by automatic image processing. *International Journal of Fracture*, 78(1), 35-44.